

**Scalable approach to generation of large symmetric Dicke states**

Sachin Kasture\*

*AMOLF, Science Park 104, 1098 XG Amsterdam, The Netherlands*

(Received 29 October 2017; published 27 April 2018)

Symmetric Dicke states represent a class of genuinely entangled multipartite states with superior resistance to loss and entanglement characteristics, even for low fidelity. A scalable and resource-intensive method is proposed using hybrid spatiotemporal encoding using only linear optics for generation of all symmetric Dicke states for both atomic and photonic qubits. Compared to purely spatial encoding, this method shows orders-of-magnitude improvement in success probability while also reducing the hardware complexity by a factor  $N$  for  $N$  qubits. This scheme will allow scalable entanglement generation of distant qubits.

DOI: [10.1103/PhysRevA.97.043862](https://doi.org/10.1103/PhysRevA.97.043862)**I. INTRODUCTION**

In his seminal paper on cooperative spontaneous emission by two-level systems [1], Dicke first described how a large number of dipole emitters could be made to behave in a correlated and coherent way via coupling to a common light field. These cooperative quantum states of emitters are now known as Dicke states. These states thus represent a possibility where distant emitters may show cooperative behavior even though they are not directly interacting with each other. In a spin-1/2 system, Dicke states are defined as the simultaneous eigenstates of both the total spin operator  $\hat{S}^2$  and its  $z$  component  $\hat{S}_z$  [1].

Besides showing interesting properties, such as superradiance [2] and spin squeezing [3], a certain class of Dicke states known as symmetric Dicke states have shown to have interesting properties for quantum-information-like multipartite entanglement, which is a valuable resource for several quantum information protocols and quantum computation algorithms. In particular, some symmetric Dicke states, which also include  $W$  states, have been shown to display properties of genuine entangled multipartite states [4]. Additionally, their entanglement is robust under particle loss compared to Greenberger-Horne-Zeilinger (GHZ) states. For example, it has been shown that for a three-qubit system, the  $W$  state retains maximal bipartite entanglement when any one of the three qubits is traced out [5], unlike for the GHZ state. It has also been shown that the required fidelity to detect genuine multipartite entanglement for large symmetric Dicke states is around 1/2 [4], unlike for  $W$  states.

Several entanglement generation schemes have been suggested in the past for entangling two atoms [6–9], as well as for entangling large macroscopic ensembles [10,11]. These schemes rely on applying a feedback to the systems for certain measurement outcomes and are probabilistic. In particular, several proposals to generate Dicke states have been discussed in literature. Reference [12], for example, uses realization of trapped ions using an adiabatic process, while [13] discusses

creating Dicke states using detection of single photons from a cavity and can be used to create Dicke states of multiple atoms inside a cavity. Reference [14] discusses a way to create Dicke states in the circuit QED framework in the ultrastrong coupling regime. References [15] and [16] are particularly interesting as they discuss a theoretical proposal for creating all the symmetric Dicke states using only linear optics. This work relies on using far-field detection of photons emitted by a group of emitters by placing detectors in a certain way and eliminating the Welcher-Weg information to project the emitters into symmetric Dicke states. Reference [17] also discusses a scheme based on linear optics and classical interference on a detector to remove which-path information and use it to create a two-qubit entangled state. Reference [18] discusses an interesting scheme to entangle two qubits using redundancy and measurements on a mutually unbiased basis. Even if an entanglement generation using a two-qubit gate fails, the qubits are not destroyed because of redundancy and the gate operation can be implemented until it succeeds. Although this scheme has the potential for deterministic entanglement, it still relies on sequential implementation of several probabilistic two-qubit gates, which means decoherence of qubits could be an issue. The scheme discussed in this work, though probabilistic, can be used to create multipartite entanglement in a single coincidence measurement.

Experimentally, an eight-qubit  $W$  state has been prepared with trapped ions inside a single cavity [19]. Experimental generation of six-photon Dicke states has been shown in Refs. [20] and [21] with fidelities of 65% and 56%, respectively, where spontaneous parametric down-conversion (SPDC) crystal in a cavity was used and pumped with femtosecond pulses. A three-qubit  $W$  state with a high fidelity of 91% was obtained using trapped ions in Ref. [22], where quantum Zeno dynamics was used to engineer the evolution of the system. This method might eventually lead to deterministic generation of entangled Dicke states, although it relies on trapping of several atoms or ions in a single cavity with the ability to perturb every emitter individually, which is experimentally very challenging. Also, this method relies on direct interaction of all the ions, while the methods discussed in the manuscript allow the entanglement of distant emitters with no direct interaction. In this article we

\*sachinkasture84@gmail.com

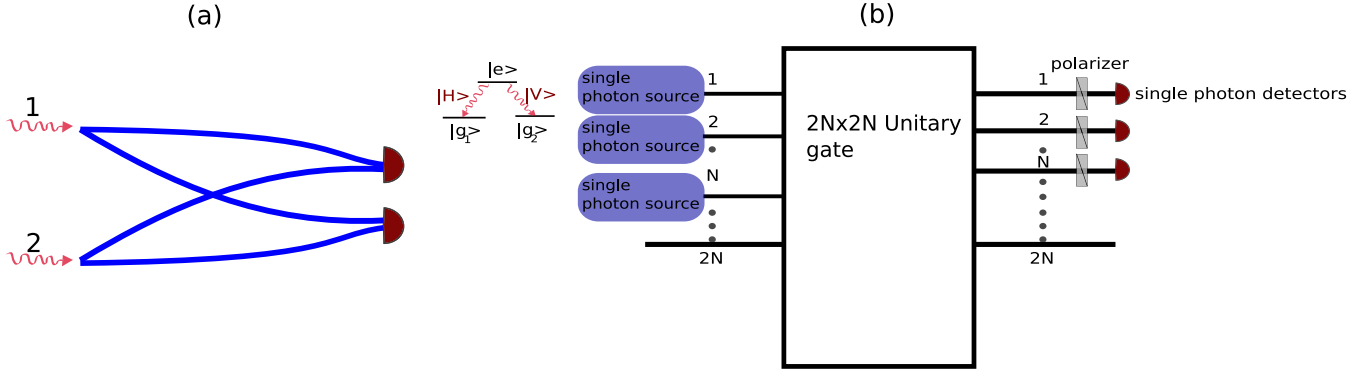


FIG. 1. (a) Nonscalable implementation of matrix in Eq. (7). (b) Scalable implementation of a  $N \times N$  nonunitary matrix using a  $2N \times 2N$  unitary matrix which can be implemented using beam splitters and phase shifters. Polarizers at the end can be used to select a particular symmetric Dicke state, as discussed in the text.

propose an approach where we can create all the symmetric  $N$ -qubit Dicke states using gates based on linear optics elements using a spatial and hybrid spatiotemporal encoding approach. Besides just relying on linear optics elements, such as beam splitters and phase shifters, this approach can be implemented using an integrated optics platform using waveguides or optical fibers, unlike for the approach used in Ref. [15]. This allows for dedicated cavities being used for individual emitters which can be used to efficiently collect and direct photons towards individual dedicated fibers. Approaches using multiports like in Ref. [23] have been proposed in the past to create  $W$  states. However, these methods fail for certain values of  $N$ . For example for  $N = 6$  and  $N = 12$ ,  $W$ -state generation is not permitted due to destructive quantum interference. The proposed method does not suffer from this limitation and may be used to generate all the symmetric Dicke states and not just the  $W$  states. Moreover, the possibility of using this approach in an integrated optics platform opens the prospect of producing multipartite entangled states for quantum emitters of different kinds (such as different quantum dots which are not usually identical or different species of ions) using intermediate quantum frequency conversion processes in waveguide-based devices [24–29]. In the next sections we first discuss a scheme to generate Dicke states based on multiports and spatial encoding. We then propose and demonstrate an approach based on hybrid spatiotemporal encoding, which greatly increases the success rate for entanglement generation while significantly reducing the resource and the hardware complexity overhead, instead relying on fast switches. In the end we discuss how all the discussed approaches may be used to generate photonic symmetric Dicke states using single-photon sources.

## II. THEORY

A general symmetric Dicke state is usually written as

$$\left| \frac{N}{2}, m \right\rangle = \binom{N}{\frac{N}{2} + m}^{-1/2} \sum_k P_k (|1_1, 1_2, \dots, 1_{N/2+m}, 0_1, 0_2, \dots, 0_{N/2-m}\rangle), \quad (1)$$

where  $N$  is the number of qubits and  $m\hbar$  is the eigenvalue of  $\hat{S}_z$  for this state. We first look at the case of a four-qubit system.

We model our qubit as a lambda system as shown in Fig. 1(a). Every transition corresponds to a different polarization for an emitted photon. For example, we could consider the transition to state  $|g_1\rangle$  corresponding to a  $|H\rangle$  for the emitted photon and  $|g_2\rangle$  to the  $|V\rangle$  photon. Also,  $|g_1\rangle$  corresponds to  $|0\rangle$  and  $|g_2\rangle$  corresponds to  $|1\rangle$  in the above equation. A typical multiport approach to create a four-qubit system would be to use a  $4 \times 4$  unitary matrix with four input and four output ports. In front of every output port one would have a polarizer to select the polarization of the output photon. One would then look at various coincidences to project the four qubits into different states. A  $4 \times 4$  symmetric unitary matrix in the spatial basis is given by

$$\begin{bmatrix} 1/2 & 1/2 & 1/2 & 1/2 \\ 1/2 & i/2 & -1/2 & -i/2 \\ 1/2 & -1/2 & 1/2 & -1/2 \\ 1/2 & -i/2 & -1/2 & i/2 \end{bmatrix}. \quad (2)$$

Now suppose  $a_{Hn}^\dagger$  and  $a_{Vn}^\dagger$  are the input operators and  $b_{Hn}^\dagger$  and  $b_{Vn}^\dagger$  are the output operators, where  $n$  is the port number, and we look at the situation where we detect an  $H$  photon in ports 1,2 and a  $V$  photon in ports 3,4. Therefore we look at the output state

$$b_{H1}^\dagger b_{H2}^\dagger b_{V3}^\dagger b_{V4}^\dagger |0\rangle. \quad (3)$$

By converting these operators into the input operators we obtain the following terms considering only those terms with one photon in each port:

$$\begin{aligned} & a_{H1}^\dagger a_{H2}^\dagger a_{V3}^\dagger a_{V4}^\dagger (1+i)(1+i) + a_{H1}^\dagger a_{H4}^\dagger a_{V2}^\dagger a_{V3}^\dagger (1-i)(1-i) \\ & + a_{V1}^\dagger a_{V4}^\dagger a_{H2}^\dagger a_{H3}^\dagger (i-1)(i-1) \\ & + a_{V1}^\dagger a_{V2}^\dagger a_{H3}^\dagger a_{H4}^\dagger (1+i)(1+i). \end{aligned} \quad (4)$$

This is equivalent to projecting the four qubits into the state

$$\frac{1}{2} (|g_{11}g_{12}g_{23}g_{24}\rangle - |g_{11}g_{22}g_{23}g_{14}\rangle - |g_{21}g_{12}g_{13}g_{24}\rangle + |g_{21}g_{22}g_{13}g_{14}\rangle). \quad (5)$$

The terms

$$a_{H1}^\dagger a_{H3}^\dagger a_{V2}^\dagger a_{V4}^\dagger, \quad a_{V1}^\dagger a_{V3}^\dagger a_{H2}^\dagger a_{H4}^\dagger \quad (6)$$

cancel out due to destructive interference. Hence the projected state in Eq. (5) is not the symmetric Dicke state. We thus see that with the symmetric unitary multiport approach it is not possible to obtain all the symmetric Dicke states. We can see that to obtain all the symmetric Dicke states, the ideal transformation matrix would be for the two-qubit case:

$$\frac{1}{\sqrt{2}} \begin{bmatrix} \frac{1}{\sqrt{2}} & \frac{1}{\sqrt{2}} \\ \frac{1}{\sqrt{2}} & \frac{1}{\sqrt{2}} \end{bmatrix}, \tag{7}$$

and for the four-qubit case,

$$\frac{1}{2} \begin{bmatrix} \frac{1}{2} & \frac{1}{2} & \frac{1}{2} & \frac{1}{2} \\ \frac{1}{2} & \frac{1}{2} & \frac{1}{2} & \frac{1}{2} \\ \frac{1}{2} & \frac{1}{2} & \frac{1}{2} & \frac{1}{2} \\ \frac{1}{2} & \frac{1}{2} & \frac{1}{2} & \frac{1}{2} \end{bmatrix}. \tag{8}$$

However, these are not unitary matrices and it is not straightforward to implement them using standard unitary multiports. The ideal way to implement this matrix would be to use an approach as shown in Fig. 1(a). Of course it would be necessary that the path lengths from every source to every detector are all equal so that there are no phase differences. However, we see that this requires  $N$  inputs and  $N^2$  outputs and quickly becomes impractical to implement and is not scalable.

We instead use another approach and embed these nonunitary matrices of size  $N \times N$  into a unitary matrix of size  $2N \times 2N$ . This can be done using the following theorem. Suppose we want to implement the nonunitary square matrix  $A$  of order  $N \times N$ ; then the unitary matrix of order  $2N \times 2N$  is given by [30]

$$\begin{bmatrix} A & (I_n - AA^\dagger)^{1/2} \\ (I_n - A^\dagger A)^{1/2} & -A^\dagger \end{bmatrix}, \tag{9}$$

where the spectral norm of  $A \leq 1$ . Using this theorem, we construct unitary matrices of size  $2N$  with a required embedded nonunitary matrix of size  $N$  and use the fact that all the sources and the detectors are in the first  $N$  input ports. The matrices for  $N = 4$  are given by

$$\frac{1}{4} \begin{bmatrix} 1 & 1 & 1 & 1 & 3 & -1 & -1 & -1 \\ 1 & 1 & 1 & 1 & -1 & 3 & -1 & -1 \\ 1 & 1 & 1 & 1 & -1 & -1 & 3 & -1 \\ 1 & 1 & 1 & 1 & -1 & -1 & -1 & 3 \\ 3 & -1 & -1 & -1 & -1 & -1 & -1 & -1 \\ -1 & 3 & -1 & -1 & -1 & -1 & -1 & -1 \\ -1 & -1 & 3 & -1 & -1 & -1 & -1 & -1 \\ -1 & -1 & -1 & 3 & -1 & -1 & -1 & -1 \end{bmatrix}. \tag{10}$$

Using the approach in Ref. [31], we can construct a linear optical circuit as shown in Fig. 1(b). We now see why with this method we can generate all the symmetric Dicke states using the transformation matrix as in Eq. (10). On detecting  $k$  photons in state  $|H\rangle$  and  $N - k$  photons in state  $|V\rangle$ , the input state is projected into the state,

$$\frac{1}{C} (a_{H1}^\dagger + a_{H2}^\dagger + \dots + a_{HN}^\dagger)^k \times (a_{V1}^\dagger + a_{V2}^\dagger + \dots + a_{VN}^\dagger)^{(N-k)} |0\rangle, \tag{11}$$

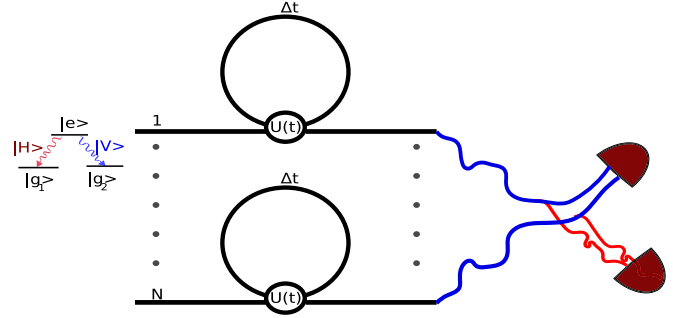


FIG. 2. Schematic for hybrid spatiotemporal approach. A lens can be used to focus light from various channels into a single spatial mode on each detector.

where  $C$  is a suitable normalization factor. We can see why the above term gives symmetric Dicke states. We only consider terms where there is only one photon in each port and use the theorem for multinomial expansion,

$$(x_1 + x_2 + \dots + x_m)^n = \sum_{k_1 + \dots + k_m = n} \frac{n!}{k_1! k_2! \dots k_m!} x_1^{k_1} x_2^{k_2} \dots x_m^{k_m}. \tag{12}$$

In our case where we want to detect one photon in each channel, each of  $k_1, k_2, \dots, k_m$  can be 0 or 1, since each channel will have a photon with either  $H$  or  $V$  polarizations. Hence the coefficient after the summation sign in the above equation will be the same for all terms, which will be  $k!$  for  $H$  polarizations and  $(N - k)!$  for  $V$  polarizations. From this we see that each term with  $N$  photons has the same amplitude coefficients. Also, the total number of terms is basically just the number of ways in which  $k$  photons in  $|H\rangle$  can be chosen from  $N$ .

The current approach uses  $O((2N)^2)$  beam splitters, where  $N$  is the number of qubits in the Dicke state. While using this method the production of Dicke states is now scalable, so it would be desirable to improve the probability of  $N$ -fold coincidences at the output, which is currently  $(N!)^2 \frac{1}{N^{2N}}$  for  $N$  identical input photons, where  $1/N$  is the maximum amplitude for a single photon in the input to reach a particular detector, which is limited by the spectral norm as required by the theorem in Eq. (9).

We now consider an approach using time bins and switching where we significantly enhance the probability of success while also reducing the hardware complexity significantly. This approach uses only delay lines, a switch and time-bin encoding to efficiently generate all symmetric Dicke states. This scheme is based on the schematic shown in Fig. 2. The input switch is used to guide emitted photons from  $N$  different emitters sequentially into  $N$  different channels. Each channel consists of a single delay line splitter whose splitting ratio is a function of time given by  $U(t)$  [32]. The delay line introduces a delay of time  $\delta t$ . The switch changes state in time less than  $\delta t$ . For example, for the case of  $N$  emitters, the state of a single photon in any given channel will be given by

$$|\psi_i\rangle = \left( \frac{1}{\sqrt{N}} \right) \sum_{j=0}^{N-1} |1\rangle_{j\delta t}, \tag{13}$$

where  $j\delta t$  correspond to different time bins. To get a symmetric superposition in the time bins for say the case of  $N = 4$ , the splitters in each spatial port should have the following unitary transformations:

$$\begin{bmatrix} \frac{1}{2} & \frac{\sqrt{3}}{2} \\ \frac{\sqrt{3}}{2} & -\frac{1}{2} \end{bmatrix}, \begin{bmatrix} \sqrt{\frac{2}{3}} & -\sqrt{\frac{1}{3}} \\ \sqrt{\frac{1}{3}} & \sqrt{\frac{2}{3}} \end{bmatrix}, \begin{bmatrix} \sqrt{\frac{1}{2}} & -\sqrt{\frac{1}{2}} \\ \sqrt{\frac{1}{2}} & \sqrt{\frac{1}{2}} \end{bmatrix}, \begin{bmatrix} 0 & 1 \\ 1 & 0 \end{bmatrix} \quad (14)$$

at intervals of time less than  $\delta t$ . However, at this stage it is still possible to identify which photon is in which time bin if we place a detector at the end of every spatial channel. To get rid of this information, we now collect photons from each channel and direct them all to a single detector, either by means of an optical fiber or by using a lens, while making sure the optical path length from each channel to the detector is the same. This is similar to the approach suggested in Ref. [15], where the authors have proposed a scheme of connecting  $N$  sources to  $N$  single-photon detectors using  $N^2$  optical fibers to get rid of the information of the source of a single photon for every detector. In our scheme, on the other hand, we use only two detectors and  $2N$  optical fibers which connect  $N$  spatial channels to the two detectors corresponding to two different polarizations. Thus now, if the detector detects a photon, it cannot identify the source of the photon. We now look for events where one photon is detected in every time bin. Since a photon from each source has an equal amplitude to be in every time bin, the emitters are projected into a symmetric Dicke state. Suppose now we have a  $\Lambda$  system where each transition also corresponds to different polarizations. The detection of a photon in the  $i$ th time bin corresponds to the following unnormalized projection operator:

$$\hat{P}_{i\Delta t} = \sum_{j=0}^N |g\rangle\langle e_j|, \quad (15)$$

where  $|g\rangle$  can correspond to  $|g_1\rangle$  or  $|g_2\rangle$  depending on detection of a  $|H\rangle$  or  $|V\rangle$  photon. After  $N$  such detections, the  $N$  atoms with initial state  $|e_1 e_2 \dots e_N\rangle$  are projected into the various symmetric Dicke states [15].

We can implement the detection setup as shown in Fig. 2, where we split the final output into two channels using a polarizing beam splitter and direct them into two different single-photon detectors. Similar to the cases discussed above, by choosing  $k$  detections for  $H$  polarization and  $N - k$  detections for  $V$  polarization, we can project the emitters into various symmetric Dicke states. To characterize the  $N$ -fold coincidence probability, we look at the situation where the input is a state with one photon of the same polarization in each of the  $N$  ports. For  $N$  input photons and  $N$  time bins the probability of detecting a photon in every time bin is given by  $\frac{N!}{N^N}$ . To see this the state after the time-bin stage is given by

$$|\psi\rangle_{n,t_n} = \left(\frac{1}{\sqrt{N}}\right)^N (\hat{a}_{1,t_1}^\dagger + \hat{a}_{1,t_2}^\dagger + \dots + \hat{a}_{1,t_N}^\dagger) \dots (\hat{a}_{N,t_1}^\dagger + \hat{a}_{N,t_2}^\dagger + \dots + \hat{a}_{N,t_N}^\dagger), \quad (16)$$

where the creation operator  $\hat{a}_{n,t_n}^\dagger$  creates a photon in port  $n$  and time bin  $t_n$ , and there are  $N$  product terms in the right side of the equation. By focusing all the spatial channels on a

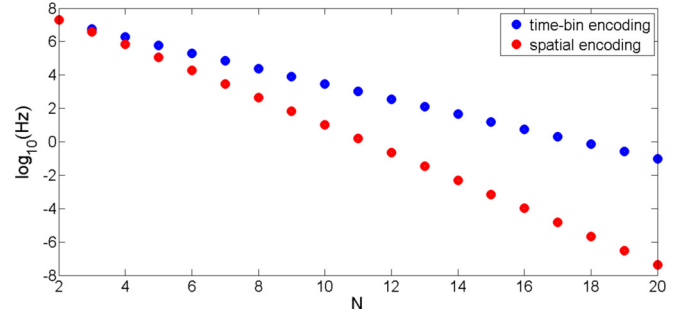


FIG. 3. Coincidence rates for different schemes using expressions given in text. The y axis plots the log-base 10 of the calculated rate in Hz.

single spatial mode on a single detector, we effectively get rid of the spatial index in the above equation and the output state becomes

$$|\psi\rangle_{\text{out}} = \left(\frac{1}{\sqrt{N}}\right)^N (\hat{a}_{t_1}^\dagger + \hat{a}_{t_2}^\dagger + \dots + \hat{a}_{t_N}^\dagger) \dots \times (\hat{a}_{t_1}^\dagger + \hat{a}_{t_2}^\dagger + \dots + \hat{a}_{t_N}^\dagger). \quad (17)$$

If we expand the right-hand side of the equation and look at terms corresponding to exactly one photon in each temporal channel, it can be seen that the probability of one photon being detected at each time bin is  $\frac{N!}{N^N}$ . A scheme which uses focusing of light from different sources on a single detector to get rid of spatial information has been shown in Ref. [17]. However, this scheme discusses the case of two qubits and does not use time-bin encoding with loop architecture, which is vital to the current scheme for hardware scalability for  $N$  qubit entanglement. For a practical situation where most single-photon detectors can only resolve pulses separated by a few nanoseconds, for a standard 80-MHz laser, one would have to wait  $N$  pulse durations before the next set of single photons arrive. This would lower the coincidence rate to  $\frac{N!}{N^{N+1}}$ . However, with faster single-photon detectors coming up (picosecond speeds), it should be possible to reach the maximum possible coincidence rate in the near future. The delay scheme is easier to implement in fibers, although ultralow loss delay lines have been demonstrated on an on-chip platform as well. Gigahertz switching speeds have been demonstrated, which should be fast enough to switch between pulses separated by a few nanoseconds. In addition to providing high success probability, this scheme has a very small hardware footprint, requiring a  $N$  delay lines,  $N$  fast switches, and one or two detectors. Additionally, this scheme can be used not only for  $N$  qubits but for  $k$  qubits, where  $k$  goes from 1 to  $N$ , with optimal success probability  $\frac{k!}{k^{k+1}}$  for each. This can be done by choosing  $k$  spatial and time-bin channels and adjusting the dynamic  $U(t)$  so that an equal superposition is created for  $k$  time bins.

Figure 3 shows the coincidence probability for different schemes for an 80-MHz pulse train. The spatiotemporal approach gives a much higher coincidence rate compared to spatial encoding. We see that by using time bins we can increase the coincidence rate significantly (orders of magnitude at large  $N$ ), at the cost of including switches and delay lines. In addition, compared to the spatial encoding approach where

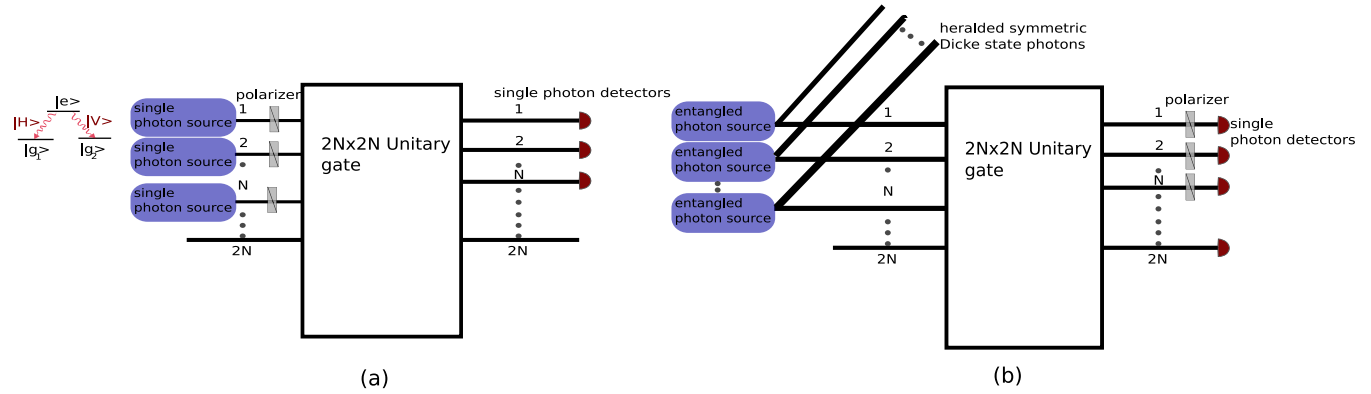


FIG. 4. (a) Generation of photon Dicke states in a postselective manner. (b) Heralded generation of photonic Dicke states using entangled sources.

the number of points of interference is  $O(4N^2)$ , the number of interference points is limited to  $O(N)$ . Also one can decide to use fewer (say  $N/2$ ) delay loops with switches while sending photons in two sets of  $N/2$  at a time, while at the output we can separate these two sets using a switch to adjust the path lengths so that all photons reach the detector at the same time. However, this will decrease the coincidence rate to  $\frac{N!}{2^{N^{N+1}}}$  but will also reduce the number of active switching components and delay lines.

We can also use this quantum circuit to generate all the symmetric Dicke states in photons. Reference [20] uses a linear optics approach to generate Dicke states by a specially designed SPDC cavity. However, the scheme in Fig. 4(a) can be used to obtain all the symmetric Dicke states using single photons from a  $\Lambda$  system. Notice the polarizers have now been placed in front of the individual emitters instead of the detectors. By choosing a definite orientation for the input polarizers, one can choose the number of  $|H\rangle$  and  $|V\rangle$  photons. However, since our gate eliminates the which-path information, on detection of  $N$  photons the output states are entangled. Figure 4(b) shows another approach for heralded generation of Dicke states using an entangled source. The setup works similar to Fig. 4(a), except that we can herald the generation of Dicke-state photons using  $N$  photon detections at the output. Similarly for the time-bin approach, we can now place polarizers in each input channel and remove the polarizing beam splitter at the output and use only one detector. On detecting  $N$  photons in  $N$  time bins, we can project the detected state into a symmetric Dicke state. By using an entangled source at the input and using the setup as in

Fig 4(b), we can also herald the generation for symmetric photon Dicke states.

### III. CONCLUSION

We have shown schemes based on spatial and hybrid spatiotemporal approaches for generation of Dicke states. These schemes are realizable in an integrated platform using on-chip waveguides or optical fibers and are scalable. We have also calculated and shown the device complexity and  $N$ -photon coincidence probability for different schemes. Additionally, this scheme allows the possibility to use dedicated optical fibers to efficiently collect photons from each individual emitter, which means multiple distant emitters can be entangled. We see that the device complexity can be significantly reduced by using hybrid spatiotemporal approach ( $O(N)$  beam splitters compared to  $(O(4N^2))$  for spatial encoding and one or two detectors compared to  $N$  for spatial approach), while greatly increasing the success probability (several orders of magnitude for large  $N$ ). These schemes in conjunction with single-photon sources like trapped ions and quantum dots should efficiently generate large, symmetric Dicke states with current available technology. We also show how these schemes could be used to generate large photon Dicke states in both a postselected and heralded manner. In addition, this scheme presents a prominent example where hybrid spatiotemporal encoding for integrated optics offers significant advantages in both speed-up and hardware complexity compared to the more used spatial encoding.

- 
- [1] R. H. Dicke, *Phys. Rev.* **93**, 99 (1954).  
 [2] Y. K. Wang and F. T. Hioe, *Phys. Rev. A* **7**, 831 (1973).  
 [3] B. Lucke, J. Peise, G. Vitagliano, J. Arlt, L. Santos, G. Toth, and C. Klempt, *Phys. Rev. Lett.* **112**, 155304 (2014).  
 [4] G. Toth, *J. Opt. Soc. Am. B* **24**, 275 (2007).  
 [5] W. Dur, G. Vidal, and J. I. Cirac, *Phys. Rev. A* **62**, 062314 (2000).  
 [6] M. B. Plenio, S. F. Huelga, A. Beige, and P. L. Knight, *Phys. Rev. A* **59**, 2468 (1999).  
 [7] C. Cabrillo, J. I. Cirac, P. Garcia-Fernandez, and P. Zoller, *Phys. Rev. A* **59**, 1025 (1999).  
 [8] J. Hong and H.-W. Lee, *Phys. Rev. Lett.* **89**, 237901 (2002).  
 [9] X.-L. Feng, Z.-M. Zhang, X.-D. Li, S.-Q. Gong, and Z.-Z. Xu, *Phys. Rev. Lett.* **90**, 217902 (2003).  
 [10] L. M. Duan, M. D. Lukin, J. I. Cirac, and P. Zoller, *Nature (London)* **414**, 413 (2001).  
 [11] L. M. Duan, *Phys. Rev. Lett.* **88**, 170402 (2002).

- [12] R. G. Unanyan and M. Fleischhauer, *Phys. Rev. Lett.* **90**, 133601 (2003).
- [13] L. M. Duan and H. J. Kimble, *Phys. Rev. Lett.* **90**, 253601 (2003).
- [14] C. Wu, C. Guo, Y. Wang, G. Wang, X.-L. Feng, and J.-L. Chen, *Phys. Rev. A* **95**, 013845 (2017).
- [15] C. Thiel, J. von Zanthier, T. Bastin, E. Solano, and G. S. Agarwal, *Phys. Rev. Lett.* **99**, 193602 (2007).
- [16] U. Schilling, C. Thiel, E. Solano, T. Bastin, and J. von Zanthier, *Phys. Rev. A* **80**, 022312 (2009).
- [17] J. Busch, E. S. Kyoseva, M. Trupke, and A. Beige, *Phys. Rev. A* **78**, 040301(R) (2008).
- [18] Y. L. Lim, A. Beige, and L. C. Kwek, *Phys. Rev. Lett.* **95**, 030505 (2005).
- [19] H. Haffner, W. Hansel, C. F. Roos, J. Benhelm, D. C. al Kar, M. Chwalla, T. Korber, U. D. Rapol, M. Riebe, P. O. Schmidt, C. Becher, O. Guhne, W. Dur, and R. Blatt, *Nature (London)* **438**, 643 (2005).
- [20] W. Wieczorek, R. Krischek, N. Kiesel, P. Michelberger, G. Toth, and H. Weinfurter, *Phys. Rev. Lett.* **103**, 020504 (2009).
- [21] R. Prevedel, G. Cronenberg, M. S. Tame, M. Paternostro, P. Walther, M. S. Kim, and A. Zeilinger, *Phys. Rev. Lett.* **103**, 020503 (2009).
- [22] Y. Lin, J. P. Gaebler, F. Reiter, T. R. Tan, R. Bowler, Y. Wan, A. Keith, E. Knill, S. Glancy, K. Coakley, A. S. Sørensen, D. Leibfried, and D. J. Wineland, *Phys. Rev. Lett.* **117**, 140502 (2016).
- [23] Y. L. Lim and A. Beige, *Phys. Rev. A* **71**, 062311 (2005).
- [24] S. Kasture, F. Lenzini, B. Haylock, A. Boes, A. Mitchell, E. W. Streed, and M. Lobino, *J. Opt.* **18**, 104007 (2016).
- [25] L. Yu, C. M. Natarajan, T. Horikiri, C. Langrock, J. S. Pelc, M. G. Tanner, E. Abe, S. Maier, C. Schneider, S. Hoffing, M. Kamp, R. H. Hadfield, M. M. Fejer, and Y. Yamamoto, *Nat. Commun.* **6**, 8955 (2015).
- [26] S. Tanzilii, W. Tittel, M. Halder, O. Alibart, P. Baldi, N. Gisin, and H. Zbinden, *Nature (London)* **437**, 116 (2005).
- [27] R. Ikuta, Y. Kusaka, T. Kitano, H. Kato, T. Yamamoto, M. Koashi, and N. Imoto, *Nat. Commun.* **2**, 1544 (2011).
- [28] S. Ramelow, A. Fedrizzi, A. Poppe, N. K. Langford, and A. Zeilinger, *Phys. Rev. A* **85**, 013845 (2012).
- [29] H. Rutz, K.-H. Luo, H. Suche, and C. Silberhorn, *Appl. Phys. B* **122**, 13 (2016).
- [30] G. Alber, T. Beth, M. Horodecki, P. Horodecki, R. Horodecki, M. Rotteler, H. Weinfurter, R. Werner, and A. Zeilinger, *Quantum Information: An Introduction to Basic Theoretical Concepts and Experiments* (Springer, New York, 2003), p. 173.
- [31] M. Reck, A. Zeilinger, H. J. Bernstein, and P. Bertani, *Phys. Rev. Lett.* **73**, 58 (1994).
- [32] K. R. Motes, A. Gilchrist, J. P. Dowling, and P. P. Rohde, *Phys. Rev. Lett.* **113**, 120501 (2014).